Controlled Dissolution of Colossal Quantities of Nitrogen in Stainless Steel

THOMAS CHRISTIANSEN and MARCEL A.J. SOMERS

The solubility of nitrogen in austenitic stainless steel was investigated thermogravimetrically by equilibrating thin foils of AISI 304 and AISI 316 in ammonia/hydrogen gas mixtures. Controlled dissolution of colossal amounts of nitrogen under metastable equilibrium conditions was realized, with nitrogen contents as high as corresponding to an occupancy of $y_N = 0.61$ of the interstitial sublattice, *i.e.*, about 38 at. pct N. Associated with the dissolution of these unprecedented nitrogen contents in an austenitic matrix a reversible volume expansion of the austenite lattice occurred for $y_N > 0.17$. A simplistic model based on a statistical distribution of the nitride forming elements over the octahedrons constituting the solid state agrees favorably with the experimental data.

I. INTRODUCTION

TRADITIONALLY, gaseous nitriding of stainless steel has been considered bad practice or, at best, a compromise, because improving the wear resistance invariably impairs the corrosion resistance. Conventional (gaseous) nitriding is carried out at temperatures above 773 K (500 °C) and chromium reacts rapidly with nitrogen to form stable chromium nitrides (CrN). Accordingly, chromium is withdrawn from solid solution and the ability for developing the (self-repairing) oxyhydroxide-based passive film at the surface, on which the superior corrosion resistance of stainless steel is based, is lost.[1]

Since the discovery in the mid-1980s of apparent supersaturation with nitrogen of (austenitic) stainless steel achieved by plasma nitriding,[2,3] expanded austenite (also called S phase) has received much interest.[4–11] Only very recently, expanded austenite was synthesized with uniform composition and unambiguously identified as a faulted fcc phase;[12] therefore, in the present work, the designation S phase is abandoned and replaced by expanded austenite, γ_X, with X = N, C, depending on N or C as the lattice expanding interstitially dissolved element. A thermodynamic description of expanded austenite has so far not been addressed, due to the lack of data that relate the chemical potential of nitrogen to the nitrogen content. Undoubtedly, this is caused by ill-defined thermodynamics of plasma-based processes for surface engineering as hitherto applied to synthesize expanded austenite.

The increasing interest in low-temperature surface engineering of stainless steel by nitriding and carburizing relates to the technical significance of the favorable properties associated with γ_X; the wear resistance is enhanced by several orders of magnitude, without impairing, or even improving, the corrosion resistance. The passive film poses a major hindrance for gaseous nitriding of stainless steel at low temperature, because it acts as a barrier for the transfer of nitrogen and carbon from an adsorbed state (at the surface) to a dissolved state (in the solid). Plasma-based nitriding involves a removal of the passive layer and prevention of its redevelopment, by simultaneous sputter bombardment of the surface during nitriding. A recently patented method[13] combines an activation of the stainless steel surface by removal of the passive layer and preventing its redevelopment during subsequent gaseous nitriding in an ammonia-based nitriding gas by a thin Ni layer. Simultaneously the dissociation kinetics of ammonia at the surface is enhanced. A similar method has been applied for gaseous nitriding of pure iron and the formation of pore-free iron nitrides at low temperature.[14] In the present work, the objective is to prevent the development of nitrides and to obtain a controlled dissolution of nitrogen in solid solution.

Various solubilities have been reported for nitrogen in expanded austenite,[4,15–18] but these values are related only to the operating parameters of the plasma/physical vapor deposition (PVD)-based experimental setup and have no general thermodynamic significance. Both Dearnley *et al.*[17] and Shedden *et al.*[18] synthesized nitrogen containing stainless steel coatings by magnetron sputtering of AISI 316[17] or AISI 316 L[18] with a range of nitrogen contents controlled by the partial pressure of N_2[17] or the flow rate of N_2 gas.[18] Dearnley *et al.*[17] determined the composition range for nitrogen-expanded austenite to $8.6 < [N] < 48$ N/100 Me by nuclear reaction analysis, *i.e.*, the range where an fcc structure was obtained. For lower nitrogen concentration, the deposited coatings had a bcc structure and for higher nitrogen concentrations unidentifiable second phases (nitrides) were present.[17] Shedden *et al.*[18] found a maximum nitrogen content in the deposited stainless steel coatings to be approximately 40 at. pct N by (standardless semiquantitative) energy-dispersive spectrometry (EDS). In addition to obviously ill-defined thermodynamics, magnetron sputtering of nitrogen stainless steel coatings entails formation of a new material due to the inherent nature of the sputtering deposition process, *i.e.*, the atomic constituents are vaporized and deposited onto a substrate, with the implication of altered composition.

As compared to plasma nitriding, gaseous nitriding has the major advantage that the chemical potential of nitrogen in the gas phase can be controlled by adjusting the so-called

THOMAS CHRISTIANSEN, formerly Postdoctoral Student, Department of Manufacturing Engineering and Management, Technical University of Denmark, DK-2800 Lyngby, Denmark, is a Postdoctor. MARCEL A.J. SOMERS, Professor of Physical Metallurgy and Leader of the Division of Materials Science and Engineering, is with the Department of Manufacturing Engineering and Management, Technical University of Denmark. Contact e-mail: somers@ipl.dtu.dk

Manuscript submitted June 23, 2005.

nitriding potential $K_N = f_{NH_3}/f_{H_2}^{3/2}$ with f_j the fugacity of component j, which usually can be replaced by the partial pressure p_j. Provided that thermodynamic equilibrium exists between gas and solid state, the nitriding potential is directly proportional to the nitrogen activity, a_N, in the solid state,[19] through $a_N = K_T \cdot K_N$, with K_T being the temperature-dependent equilibrium constant of the dissolution reaction $NH_3 \Leftrightarrow [N]_\gamma + \frac{3}{2}H_2$ where $[N]_\gamma$ indicates nitrogen dissolved in austenite.

In the present article, the solubility for nitrogen in austenitic stainless steel and the composition dependence of the lattice parameter of homogeneous γ_N are investigated by equilibrating thin foils at various nitriding potentials. A simplified picture of the distribution of nitrogen over the octahedral sites in the fcc lattice and an estimation of the maximum lattice solubility for nitrogen are given.

II. EXPERIMENTAL

A. *Sample Preparation*

Thin foils of stainless steel AISI 304 and AISI 316, with thickness 5 and 7.5 μm, respectively, were used for nitriding. The major difference in composition between the materials (Table I) is the presence of Mo in AISI 316, accompanied by a slight reduction of the Cr content and an enhanced Ni content to compensate for the ferrite stabilizing effect inherent to the addition of Mo.

For recrystallization and transformation of deformation-induced martensite, the (cold-rolled) thin foils were austenitized by heating to 1343 K at a heating rate of 1/3 K/s. Upon reaching this temperature, the samples were immediately cooled in pure H_2. After heat treatment, the foils were pretreated to allow nitriding in an ammonia nitrogen atmosphere.[13] This pretreatment involves chemical stripping of the passive film, followed by electrochemical deposition of Ni in a Wood's nickel bath ($NiCl_2 + NiSO_4 + H_2SO_4$). The maximum thickness of the deposited layer was 20 nm, as calculated from Faraday's law and assuming an efficiency of 3 pct during electrodeposition.*

*This value is an upper estimate of empirically realized efficiencies; the remaining 97 pct of the current is used for H_2 development.

The purpose of the thin electrodeposited nickel layer is twofold: preventing the repassivation of the stainless steel surface during handling and catalyzing the dissociation of ammonia at the surface. Although the dissolution of nitrogen in the nickel layer is negligibly small, transport of N atoms through the Ni layer is determined by the chemical potential difference over this layer, which can be very large. For the present experiments (absorption isotherms), the rate of nitrogen transfer to the sample through the Ni layer was not found to play an important role.

Table I. Compositions of the Applied Stainless Steel Alloys in Atomic Percent

Alloy	Cr	Ni	Mo	Mn	Si	Fe
AISI 304	19.60	8.68	0	1.66	1.26	68.80
AISI 316	19.11	12.70	1.40	1.74	1.45	63.60

B. *Thermogravimetric Control of Gaseous Nitriding and Denitriding*

Gaseous nitriding was performed in a Netzsch STA 449C (Netzsch Gerätebau GmbH, Germany) simultaneous thermal analyzer, which allows simultaneous thermogravimetric analysis and differential thermal analysis. The following procedure was followed for controlling the nitrogen content in the stainless steel samples. Several pretreated (Ni-sheathed) foils with a total mass of typically 30 to 40 mg were supported in the sample containers (crucibles) of the apparatus. The total sample mass was limited to this value on account of the size of the sample containers.

The Ni deposit contributes to maximally 0.8 pct of the total mass for the foil with thickness 5 μm and proportionately less for the foil with thickness 7.5 μm; as mentioned previously, the solubility of nitrogen in Ni is negligibly small. A correction for the presence of the Ni deposit, which would imply higher nitrogen contents in austenite, is insignificant and was therefore omitted.

The gases led into the thermal analyzer were controlled by Brooks electronic mass flow controllers each capable of a maximum flow of 5/6 mL/s. The minimum controllable flow for each gas was 1/60 mL/s. The total flow of NH_3 and H_2 was within the range 5/6 to 5/3 mL/s. The flow of N_2 was kept constant for all experiments at 1/12 mL/s. The purity of NH_3, H_2, and N_2 was 99.9, 99.9, and 99.9999 pct, respectively.

The samples were heated to the nitriding temperature in pure ammonia and nitrogen**—reaching the nitriding temperature within 2400 seconds. Two nitriding temperatures were chosen, in accordance with the difference in thermal stability of the formed expanded austenite in the two materials; *i.e.*, a higher temperature is allowed in AISI 316.[20] Both materials were nitrided at 693 K for direct comparison; AISI 316 was also nitrided at 718 K. Nitriding was continued until the mass increase associated with nitrogen uptake in the sample was stationary, indicating saturation of the sample. The nitrogen content obtained under these conditions is the maximum solubility, provided that the dissolution of N in γ_N is not competing with the development of N_2 at the surface.[19] After saturation, the gas composition was changed to a mixture of ammonia and hydrogen in order to adjust the nitrogen content. Consequently, the foil looses nitrogen by the development of ammonia at the sample surface until a new stationary sample weight is reached. In order to correct for the influence of buoyancy effects on the quantification of the recorded weight changes, an identical temperature-time-gas composition program was run with empty crucibles. The thus obtained baseline was subtracted from the recorded weight change curve of the sample.

The relation between nitriding potential and the stationary nitrogen content in the sample at a specific temperature, a so-called absorption isotherm, was determined by reducing the nitriding potential in steps down to $K_N = 0$. In each step, a stationary sample weight was reached before the next, lower nitriding potential was adjusted.

**For protecting the balance chamber from ammonia, high-purity nitrogen was led through the measurement compartment and thereafter the nitriding compartment.

C. *X-ray Diffraction*

For determination of the lattice parameter of uniform γ_N, foils with thermogravimetrically controlled nitrogen content, the nitrided foils were powdered with ultra-sound while submerged in ethanol. Mechanical preparation of the powders from fully nitrided foils was prevented since introductory experiments had shown that this leads to a deformation-induced (partial) transformation of γ_N to martensite. The powder-ethanol slurry was smeared on a glass plate and, after evaporation of ethanol, analyzed with a Bruker AXS (Bruker AXS GmbH, Germany) D8 X-ray diffractometer, equipped with a Co anode and a set of Göbel mirrors in the incident beam. Positions of the Bragg peaks in the X-ray diffraction patterns were obtained from fitting a pseudo-Voigt peak shape function through the measured intensities forming the peak. In the fitting procedure corrections for K_{α_2}, Lorentz polarization and absorption factors were included. Since expanded austenite has a faulted fcc structure, the peak shifts associated with the presence of stacking faults were accounted for during data evaluation.[12]

III. RESULTS AND INTERPRETATION

A. *Nitrogen Solubility in Austenitic Stainless Steel*

The nitrogen solubilities corresponding to stationary sample weights for AISI 304 and AISI 316 are presented in Figure 1 as the occupancy y_N, *i.e.*, the fraction of the interstitial sublattice occupied by nitrogen atoms,* as a function of the nitrogen activity, a_N, that would apply for (imposed) equilibrium between gas and solid state. Clearly, a linear relation applies between y_N and ln a_N for nitrogen activities ranging from ln $a_N = 3$ to ln $a_N = 10$. For nitrogen activities lower than $a_N = e^3$, a stronger dependence of y_N on ln a_N applies. Upon reduction of uniformly nitrided samples in pure hydrogen, not all nitrogen atoms can be withdraw from solid solution in stainless steel. The minimum nitrogen contents attainable in AISI 304 and AISI 316 are indicated in Table II and by the horizontal lines denoted by $a_N = 0$ in Figure 1. Upon nitriding in pure ammonia, the maximum nitrogen contents attainable are indicated in Table II and by the horizontal lines denoted by $a_N = \infty$ in Figure 1. The data in Figure 1 demonstrate convincingly that colossal quantities of nitrogen can be dissolved reproducibly by imposing a nitrogen activity adjusted through the nitriding potential, K_N, of the gas mixture and the temperature of the sample.

*Nitrogen containing Fe-based phases can be conceived as constituted of a substitutional sublattice on which the metal atoms reside and an interstitial sublattice formed by the octahedral interstices of the substitutional sublattice. For an fcc lattice, the substitutional and interstitial sublattices are both fcc and have the same number of sites.

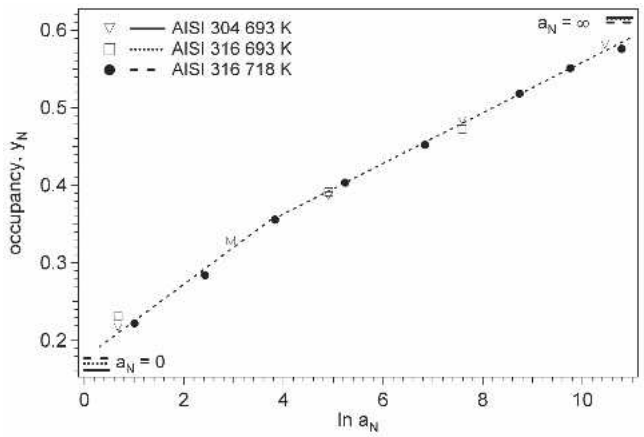

Fig. 1—Nitrogen solubility in expanded austenite, γ_N, as a function of nitrogen activity, a_N, applied for nitriding AISI 316 at 693 and 718 K and for nitriding AISI 304 at 693 K. Straight lines through the data are indicated to guide the eye. The solubility levels for the nitrogen activities nil and infinity are indicated by horizontal bars.

The minimum occupancies of the interstitial lattice after reduction in pure hydrogen are close to, but significantly lower than, the chromium content of the sample (columns indicated N:Cr in Table II). Evidently, the binding of nitrogen atoms in the sample up to the quantities denoted by $a_N = 0$ is stronger than in NH_3 molecules forming at the surface during reduction in hydrogen. It is emphasized that the present nitrogen solubilities for low nitrogen activities were obtained through stepwise denitriding of fully nitrided samples and will therefore deviate from the solubilities that may be obtained upon equilibrating austenitic steels foils immediately in an atmosphere containing a low a_N. Equilibrating the samples in an atmosphere corresponding with $a_N = \infty$ implies exceeding of the solubility limit of nitrogen (nitrogen is trapped by Cr). It is anticipated that reversible nitrogen dissolution is obtained if nitriding is carried out at low a_N where the solubility limit is not exceeded. Such experiments were not performed in the present work.

Recognizing that, of the elements present in the sample, chromium has the largest affinity for nitrogen, the lowest attainable nitrogen occupancy would be expected to equal the content corresponding to a nitrogen-to-chromium ratio N:Cr = 1:1. Since roughly speaking every sixth metal atom in the fcc lattice is a Cr atom, on average, each octahedral interstice has a Cr atom as nearest neighbor. Evidently, nitrogen atoms in excess of Cr:N = 1:1 are less tightly bound than nitrogen atoms for quantities up to this stoichiometry. The solubility of nitrogen within the range of nitriding activities depicted in Figure 1 appears to be subdivided in two regions, as suggested by different slopes (indicated to guide the eye). The slight discrepancy observed at low

Table II. Nitrogen Solubilities in Expanded Austenite, y_N, Obtained on Gaseous Nitriding of AISI 304 and AISI 316 at Temperature, T, Nitrogen Activity, a_N, Indicated*

		y_N		N:Cr		N:Cr + Mo	
AISI	T[K]	$a_N = 0$	$a_N = \infty$	$a_N = 0$	$a_N = \infty$	$a_N = 0$	$a_N = \infty$
304	693	0.162	0.616	0.826	3.14	—	—
316	693	0.170	0.615	0.891	3.22	0.831	3.00
316	718	0.177	0.610	0.926	3.19	0.863	2.97

*$a_N = 0$ refers to fully nitrided and subsequently H_2-reduced samples. Nitrogen solubilities are also given as the ratios in relation to the atomic fractions of nitride forming elements Cr and Cr + Mo in the steels (*cf.* Table I).

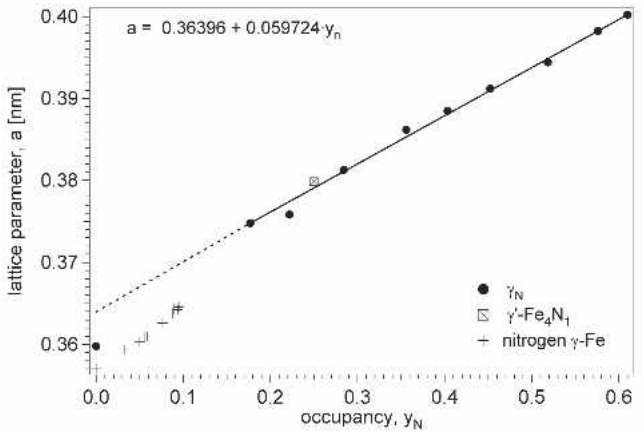

Fig. 2—Lattice parameter of homogenous expanded austenite synthesized by gaseous nitriding of AISI 316 at 718 K at various nitrogen activities.

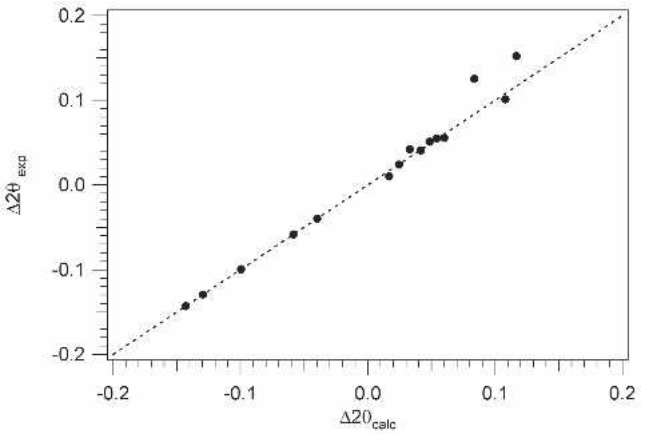

Fig. 3—Plots of experimental, $\Delta 2\theta_{exp}$, *vs* calculated, $\Delta 2\theta_{exp}$, peak shifts for homogeneous expanded austenite obtained by gaseous nitriding of AISI 316 at 718 K and various nitrogen activities. The dashed line has slope 1 and is not a linear fit to the data.

occupancies/activities is ascribed to experimental difficulties with the withdrawal of nitrogen at 693 K for AISI 316.*

*Equilibrating AISI 316 at 693 K at low nitriding potentials was sluggish compared to 718 K. Equilibrating AISI 304 at 693 K proved easier as the thickness of this material was only 5 μm compared to 7.5 μm for AISI 316. By extrapolating the thermogravimetric weight curve—assuming that the nitrogen retraction is diffusion controlled—an estimate for the error can be calculated: in the low nitriding potential range for AISI 316 at 693 K, a maximum error of $y_N = + 0.005$ may occur. Hence, the occupancy could be slightly overestimated in the low nitrogen potential range for AISI 316 at 693 K.

These distinct regions could imply that nitrogen atoms residing in the octahedral interstices experience different chemical environments. Presuming that Ni in stainless steel has a negligible effect on the dissolution of nitrogen, the presence of Mo is the only major difference between AISI 304 and AISI 316. Apparently, Mo does not influence the lattice solubility markedly for nitrogen activities up to e^{10}. Molybdenum plays a dominant role with regard to the nitriding behavior of austenitic stainless steel; in particular, it enhances the temperature stability of γ_N.[20] The influence of Mo is only apparent when N:Cr is considered at $a_N = 0$ and $a_N = \infty$; it compensates for the reduced Cr content and maintains the same N content in the alloy. A possible influence of Si and Mn cannot be discerned because the concentrations of these elements are relatively low. Furthermore, as mentioned previously, the concentrations of Mn and Si do not vary much in the investigated steels, which hinder elucidation of any trends.

B. *Lattice Parameter of Expanded Austenite*

The lattice parameter, a, of γ_N is presented as a function of the occupancy of the interstitial sublattice, y_N, in Figure 2. Evidently, for nitrogen occupancies higher than the minimum solubility close to N:Cr = 1:1, a linear relation holds between the lattice parameter, a, and y_N (Figure 2). The data suggest that the lattice expansion per nitrogen atom in the composition range up to this solubility is even more pronounced, but, for obvious reasons, no data were obtained in this regime. Literature data for nitrogen dissolved in Fe-austenite are depicted for nitrogen contents up to $y_N = 0.095$, which corroborates that a more pronounced lattice expansion per nitrogen atom exists in this regime (Figure 2).[21] As pointed out in Reference 12, dissolution of high quantities of nitrogen in γ_N is accompanied by the introduction of stacking faults in the fcc lattice. On determining the lattice parameter from the X-ray diffractograms, the stacking fault probability was incorporated into the fit procedure in order to take systematic deviations from the perfect fcc Bragg position into account. The experimentally observed deviation from the Bragg position, $\Delta 2\theta_{exp}$, is compared with the calculated value, $\Delta 2\theta_{calc}$. The excellent correspondence of the data with a line of slope = 1 (the dashed line in Figure 3) provides additional evidence for the faulted fcc structure of expanded austenite. No systematic dependence of the stacking fault probability, α, on the nitrogen content was found: α ranged from 0.01 to 0.04. A lack of such a relation is attributed to stacking fault production during nitriding; in an early stage of the nitriding process, compositional gradients and concomitant stress gradients arise in the thin foil and stress relaxation by production of stacking faults is expected to occur. Initially, the thin foils are saturated at an infinite nitriding potential before lowering the nitriding potential. During denitriding to the nitrogen concentration mentioned, compositional gradients (and thus stress gradients) arise again. Hence, the observed stacking fault probability does not necessarily reflect the "equilibrium" value for the adjusted nitrogen concentration, but is largely determined by the (stress) history of the sample.

IV. DISCUSSION

A. *Lattice Solubility*

Generally, the stationary nitrogen content in iron-based phases obtained in ammonia/hydrogen mixtures reflects a stationary state rather than a state of thermodynamic equilibrium,[19] because the dissolution of nitrogen in the solid state competes with the development of molecular nitrogen at the surface (which is preferred thermodynamically). In the present work, the stationary nitrogen contents achieved during the nitriding and denitriding experiments can be conceived as a metastable equilibrium state, rather

than a stationary state, because the development of molecular nitrogen can be neglected at the nitriding temperature. This was verified by heating saturated expanded austenite powder (at $a_N = \infty$) in an atmosphere of N_2 in order to investigate its stability: the development of N_2 did not occur for temperatures below 773 K.[20] However, austenite with a high nitrogen content is metastable with respect to CrN, ferrite, or austenite and tends to decompose (Figure 4). Effectively, for the process times usually applied for nitriding, the development of CrN from metastable expanded austenite is hindered at temperatures below, say, 723 K. This was verified by X-ray diffraction analysis and by thermal analysis of nitrogen equilibrated thin foil (*cf.* Reference 20). Presumably, this slow kinetics can be attributed to the limited mobility of substitutional alloying elements at low temperatures, as compared to the mobility of interstitial elements.

Evidently the colossal nitrogen contents in as-nitrided stainless steel are beyond the solubilities that can be expected, taking into account the possible nitrides that can develop (of which CrN will dominate) and the equilibrium lattice solubility of nitrogen in austenite (as extrapolated from data at much higher temperatures than applied in the present investigation). The solubility of nitrogen in an iron-based matrix has frequently been observed to exceed the solubility calculated from the lattice solubility and the nitrogen involved in the development of stoichiometric nitrides dispersed in the matrix, so-called excess nitrogen (for an overview, see Reference 22). An explanation for the occurrence of excess nitrogen in ferritic alloys relies on the presence of nitrogen at the interface between dispersed nitrides and the matrix and on enhanced matrix solubility due to a dilatation of the matrix caused by coherency strains of the misfitting nitrides. An analogous explanation for the colossal nitrogen solubilities observed in expanded austenite cannot apply, because no nitrides are present. Furthermore, excess nitrogen contents as high as N:M = 3:1 have so far only been reported for low temperature (673 K) nitriding of ferritic Fe-Ti alloys containing 2 at. pct Ti,[23] where the total occupancy of the interstitial sublattice of octahedral interstices is 6 N atoms per 100 metal atoms (corresponding with an occupancy of $y_N = 0.02$ of the octahedral positions in the bcc lattice). For higher nitriding temperatures, this nitrogen solubility could no longer be attained in Fe-Ti alloys. The present maximum solubilities in austenitic stainless steel are 10 times as high (about 60 N atoms per 100 metal atoms) and unprecedented for a gaseously nitrided material under imposed (metastable) equilibrium conditions.

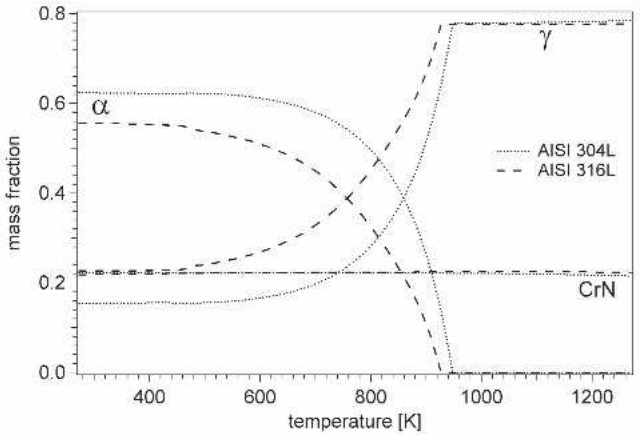

Fig. 4—Equilibrium diagram showing the thermodynamically stable phases as a function of temperature for AISI 304L and AISI 316L with a nitrogen content equivalent to the chromium content (ThermoCalc). The calculations were performed considering only fcc and bcc phases.

On comparing the homogeneity range for nitrogen solubility in stainless steel with the results given in Reference 17 ($8.6 \leq [N] \leq 48$ N/100 Me, which corresponds to $0.086 \leq y_N \leq 0.48$), a different range is obtained in the present work. This can be directly ascribed to the method of magnetron sputtering as applied in Reference 17, where the fcc structure seemingly is stable only in a certain concentration range (as stated previously). Lower and higher nitrogen contents are associated with the formation of a bcc structure and second phases, respectively. In Reference 18, a maximum nitrogen content of approximately 40 at. pct N was found, although crystallographic determination was not possible with X-ray diffraction analysis. Hence, comparison to the maximum solubility found in this work (38 at. pct) is futile due to a lack of verification of the formed structure. As mentioned earlier, magnetron sputtering as a method for synthesizing nitrogen containing stainless steel (expanded austenite) is flawed by, in particular, ill-defined thermodynamics, but also by the material's dissimilarity to heat-treated stainless steel. The distribution of (substitutional) atoms is a consequence of the heat-treatment history, *e.g.*, austenitization; magnetron-sputtered coatings may be different in this way, as the distribution of (substitutional) atoms is governed by impingement.

B. *Modeling of Lattice Solubility*

Formal models for nitrogen solubility were applied unsuccessfully. In order to obtain a reasonable description of the data by the Redlich–Kister formalism,[24] five fit parameters were required, which makes the description physically meaningless. Neither did the Wagner–McLellan cell model[25] with four fit parameters provide an accurate, physically meaningful description. The distribution of nitrogen atoms in the austenitic Fe-Ni-Cr-(Mo) alloys AISI 304 and AISI 316 is most likely governed by the distribution of the nitride forming elements. It is evident from the solubility plot in Figure 1 that several distinct regions are present, which further substantiates that different octahedral interstices are occupied in different nitrogen activity regimes. As a zeroth order approximation, it is assumed that the substitutional alloying elements are randomly distributed over the available lattice sites. This appears to be a reasonable assumption, particularly when it is taken into account that the samples were austenitized prior to nitriding. Recognizing that the number of lattice sites of the fcc host lattice equals the number of octahedral sites for nitrogen atoms, the probability, $P(n)$, that an octahedron contains n ($n = 0..6$) Cr atoms is calculated from

$$P(n) = \binom{6}{n} \cdot y_{Cr}^{n} \cdot (1 - y_{Cr})^{6-n} \qquad [1]$$

where y_{Cr} is the atomic fraction of Cr atoms. Straightforward extension of Eq. [1] gives the probability $P(n,m)$, that

an octahedron contains n Cr atoms and m (m = 0..6 − n) Mo atoms:

$$P(n,m) = \binom{6}{n} \cdot y_{Cr}^{n} \cdot \binom{m}{6-n} \cdot y_{Mo}^{n-m}(1 - y_{Cr} - y_{Mo})^{6-n-m} \quad [2]$$

where y_{Mo} is the atomic fraction of Mo atoms. The probabilities $P(n)$ and $P(n,m)$ with $n = 0..6$ and $m = 0..2$ were calculated for the composition of AISI 304 and AISI 316 (Table I), respectively, and are given in Table III.

The Cr-N interaction is relatively strong, though it is not a genuine chemical bond as in the nitride compound CrN. Due to the interaction between Cr and N, the nitrogen trapping ability of an octahedral interstice should increase when the fraction of Cr atoms (or other strong nitride formers) dissolved on the contiguous substitutional lattice is increased. However, the larger size of Cr and especially Mo compared to Fe decreases the available space for the interstitially dissolved N. Consequently, the presence of Cr atoms in the octahedron clusters will increase the probability (affinity) for nitrogen to reside in the pertaining octahedral interstices in terms of (semi) bonding, but the size/strain factor will counteract this phenomenon. Thus, it is highly likely that an intermediate situation occurs in terms of effective nitrogen affinity, due to the opposing effects of the (semi) bonding term and the size/strain term. Consequently, different energy levels of nitrogen bonding should prevail as a function of the nitriding potential.

In the present case, it is not considered likely that octahedron clusters with $n = 0$ Cr atoms are occupied with nitrogen atoms.

The calculated probabilities in Table III can be compared with values for the minimum and maximum lattice solubilities indicated by $a_N = 0$ and $a_N = \infty$, respectively (Table II). For AISI 304, a good correspondence occurs for $P(1) + P(2) = 0.635$ with $y_N = 0.616$. The probability $P(1) = 0.396$ could be associated with the onset of linearity between y_N and ln a_N. However, a limited number of data points (as compared to AISI 316) makes it difficult to ascertain this. For AISI 316, a striking agreement is found for $P(1,0) = 0.359$ and $y_N = 0.36$, where the linearity between y_N and ln a_N begins. This may indicate that the octahedrons containing only 1 Cr atom as a nitride former are effectively occupied at this nitrogen content. Summing the probabilities $P(1,0)$, $P(2,0)$, and $P(1,1)$ gives 0.606, which agrees favorably with the maximum solubility in AISI 316 of $y_N = 0.610$. Then, it appears likely that octahedrons containing 2 Cr atoms are occupied immediately after filling of those containing only 1 Cr atom. According to this scheme, another change of slope would be expected at $y_N > 0.569$ for AISI 316. No conclusive data exist to verify this. Decreasing order of probability for finding a particular octahedron with nitride forming elements shows that $P(1,0) > P(2,0) > P(3,0) > P(1,1)$. A filling of the corresponding octahedral interstices in the order $P(1,0)$, $P(2,0)$, $P(1,1)$ would be consistent with the importance of a size effect of the alloying elements Cr and Mo. Evidently, octahedral interstices having more than two nitride-forming elements as nearest neighbors are preferably not occupied by nitrogen atoms.

Table III. Probabilities $P(n)$ and $P(n,m)$ for Octahedron Configurations Containing n Cr Atoms and m Mo Atoms

	$P(n)$		$P(n,0)$	$P(n,1)$	$P(n,2)$
n	304	316	316	316	316
0	0.273	0.284	0.256	0.026	0.001
1	0.396	0.398	0.359	0.037	0.002
2	0.239	0.232	0.210	0.022	0.001
3	0.077	0.072	0.065	0.007	0.000
4	0.014	0.013	0.011	0.001	0.000
5	0.001	0.001	0.001	0.000	—
6	0.000	0.000	0.000	—	—

The maximum solubility observed in AISI 304 or AISI 316 is governed by two main factors: (1) the energy release associated with the chemical reaction(s) occurring at the surface, and the subsequent interstitial dissolution of N in the lattice, and (2) the strain energy contribution caused by a dilation of the metal matrix by misfitting nitrogen atoms. The balance between total energy release and energy increase in strain energy depends on the immediate surroundings of the octahedral interstice in which a nitrogen atom is located. Effectively, the maximum capacity for dissolved nitrogen atoms in a sample can be considered the outcome of these antagonistic energy contributions.

It should be recognized that the preceding interpretation is not rigorous and that for occupancies of the interstitial sublattice the influence of next-nearest neighbors has to be taken into account. Likewise, the role of Ni, Si, and Mn atoms in the octahedrons is anticipated to play an important role.

C. *Lattice Expansion*

The relationship between lattice parameter and nitrogen concentration was in this work found to be linear within the homogeneity range of nitrogen-expanded austenite. For comparison, the lattice parameter of γ'-Fe_4N is given. This compound has an fcc lattice of Fe atoms and the N atoms are distributed according to strict long-range order over the octahedral interstices, *i.e.*, one per fcc unit cell. Evidently, the lattice parameter of γ' nitride is in very good agreement with the dependency found for γ_N. This suggests that the lattice parameter of iron-based phases with a high content of nitrogen is largely governed by the misfitting of nitrogen atoms in the octahedral interstices. In Reference 17, a relationship for the lattice parameter as a function of composition within the range $0.086 \leq y_N \leq 0.48$ was found as $a = 0.3585 + 0.00075$ [N] nm, which deviates considerably from the lattice dilation determined in the present work. This discrepancy can partly be ascribed to sample preparation by magnetron sputtering in a nitrogen gas atmosphere, which suffers from ill-defined thermodynamics for nitrogen solubility and elemental distribution during coating deposition. In this respect, the limited range associated with formation of an fcc structure (*i.e.*, expanded austenite) demonstrates the unsuitability for applying such a process for determination of the lattice parameter as a function of composition in stainless steel. Moreover, determining the lattice spacing with X-ray diffraction methods for a coating on a substrate is significantly influenced by residual stress in the coating. For such high nitrogen contents (up to 40 at. pct), the contribution of stresses on the measured lattice parameter can be significant. Additionally, stacking faults, inherent to

expanded austenite, will also give rise to a systematic lattice parameter deviancy, if not corrected for (in Reference 17, such a correction was indeed omitted). A similar argument applies for the discrepancy between the present lattice dilation and the relation given by Shedden *et al.*[18] In addition, the semiquantitative character of the (EDS determined) nitrogen contents and application of the crystallite-group method for lattice parameter determination—which, erroneously, presumes elastic isotropy for austenite—from two lattice spacings contribute to this discrepancy.

D. *Practical Implications of Dissolution of Nitrogen in Stainless Steel*

The experimental results presented in this article for homogeneous thin foils show the thermodynamically feasible nitrogen contents for equilibrium between a gas mixture of controlled composition and the nitrogen content in solid solution in austenitic stainless steel. In this sense, the results show that the nitrogen content can be accurately adjusted by controlling the activity of nitrogen of the gas mixture. Transferring the present results to practice, where generally only the surface of stainless steel will be treated, is not straightforward. Reflected light micrographs of cross sections of nitrided AISI 316 bulk samples are shown in Figure 5 for two different nitriding potentials (the caption for Figure 5 provides details).

Clearly, the nitrided zone has a seemingly sharp interface with the substrate, suggesting separate phases in layer and substrate. However, X-ray diffraction analysis of these samples (not shown here) only shows the occurrence of expanded austenite, albeit with asymmetric line profiles owing to a depth gradient of the nitrogen content. Microstructural features as grain and twin boundaries extend from the bulk into the layer, suggesting that the layer indeed consists of the same host lattice. It is anticipated, and preliminary results of modeling actual nitrogen concentration-depth profiles confirm,[26] that the "interface" marks the nitrogen concentration above which a strong bonding between Cr and N atoms occurs (*i.e.*, nitrogen that cannot be removed by a reduction in streaming hydrogen; Section III–A). One could expect that for nitriding thick samples, the thermodynamic equilibrium situation as obtained for the thin foils is, at best, only achieved at the surface. A direct comparison between equilibrium nitrogen contents at the surface of the bulk and in equilibrated homogeneous thin foil samples is not allowed. The following two conditions illustrate why such a comparison is invalid. In bulk samples, high compositionally induced compressive stress values are anticipated to have an influence on the actual equilibrium lattice solubility, *i.e.*, the thermodynamics of stressed solids should be taken into account.[27] For a particular nitrogen activity, both the competition between ammonia dissociation and solid-state diffusion as well as the large compositionally induced compressive stresses lead to lower nitrogen contents for the surface of bulk samples as compared to stress-free thin foils of uniform composition.

The concentration of adsorbed nitrogen atoms, which is anticipated to be in equilibrium with the composition of the surface of the bulk substrate, is determined by the competition of nitrogen atoms arriving at the surface as a consequence of the dissociation of ammonia and nitrogen atoms diffusing into the interior of the sample. As was shown for ferritic surfaces, the dissociation reaction of ammonia is relatively slow[19,28] and indeed competes with the inward diffusion of nitrogen atoms. No such data are available for the present case.

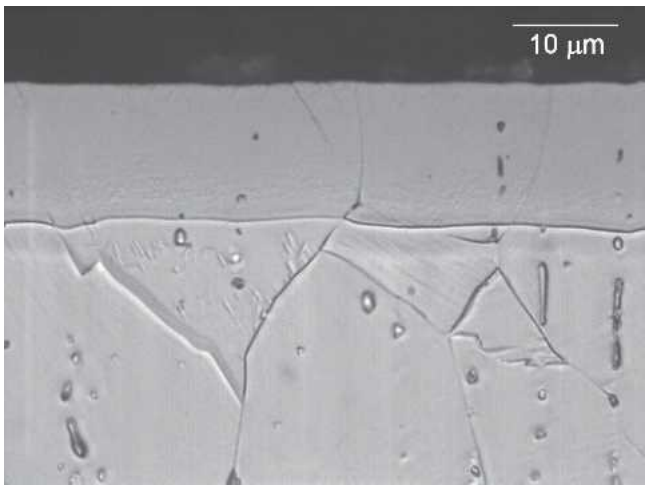

(*a*)

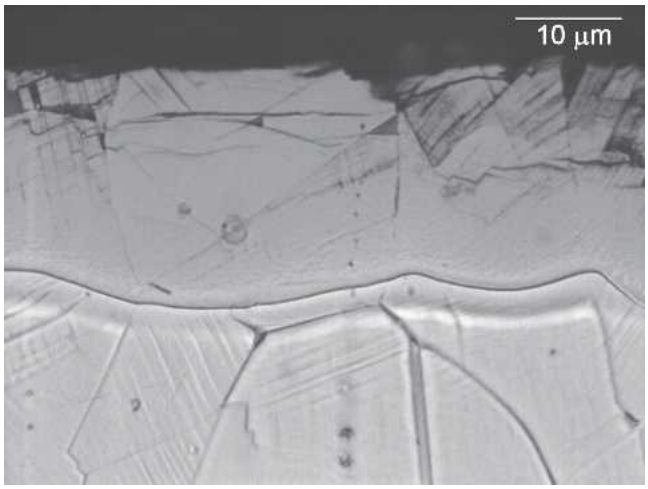

(*b*)

Fig. 5—Reflected light micrographs of cross sections of nitrided AISI 316. Nitriding temperature and time were 718 K and 22 h, respectively, for both samples. The nitriding potentials were (*a*) $K_N = 2.49\ \text{bar}^{-1/2}$ ($\ln a_N = 5.78$) and (*b*) $K_N = \infty$ ($\ln a_N = \infty$). The cross sections were etched in a mixture of 50 vol pct HCl, 25 vol pct HNO_3, and 25 vol pct H_2O.

The technological importance of thermochemically treated strainless steel is surface hardening without impairing the corrosion properties. Since the actual hardening is associated with an interstitial solid solution of nitrogen (carbon) in an austenitic lattice, the main strengthening mechanism is expected to be solid solution strengthening. Hardness depth profiles in nitrided bulk samples reflect a relatively sharp drop in hardness at the transition from expanded austenite to un-nitrided austenite together with a plateau in the near-surface region. Hardness values in excess of more than 1500 HV (as compared to a bulk hardness of 250 HV) are not uncommon for high nitrogen contents.[29]

The significance of controlling the nitrogen content in expanded austenite layers by adjusting the gas composition

is obvious from Figure 5. Excessively high nitrogen contents can induce cracking of the expanded austenite layer (Figure 5(b)). An X-ray diffraction–based determination of lattice strains by the so-called $\sin^2 \psi$ method indicates that these stresses can amount to -7 to -8 GPa's and that cracking is indeed associated with stress relaxation.[30]

V. CONCLUSIONS

Controlled dissolution of colossal quantities of nitrogen in stainless steel is possible by applying gaseous nitriding. The process of gaseous nitriding enables control of the nitrogen activity because nitriding is carried out in a controlled atmosphere of NH_3/H_2. Nitrogen solubility plots were obtained for both AISI 304 and AISI 316 for the full range of possible nitrogen activities. The homogeneity range of expanded austenite spans from an interstitial occupancy of $y_N = 0.177$ to $y_N = 0.610$ for AISI 316 at 718 K. A similar range was obtained for AISI 304 and AISI 316 at 693 K. A simplistic model based on a statistical distribution of the nitride forming atoms is in conformity with the experimental data. The lattice parameter of expanded austenite was determined and proved to be a linear function of nitrogen concentration within the homogeneity range.

ACKNOWLEDGMENT

Financial support by the Danish Research Agency under Grant No. 26–01-0079 is gratefully acknowledged.

REFERENCES

1. *ASM Specialty Handbook: Stainless Steel*, ASM International, Metals Park, OH, 1994.
2. Z.L. Zhang and T. Bell: *Surf. Eng*., 1985, vol. 1 (2), pp. 131-36.
3. K. Ichii, K. Fujimura, and T. Takase: *Technol. Rep. Kansai Univ*., 1986, vol. 27, pp. 135-44.
4. D.L. Williamson, O. Ozturk, R. Wei, and P.J. Wilbur: *Surf. Coating Technol*., 1994, vol. 65, pp. 15-23.
5. M.K. Lei and Z.L. Zhang: *J. Vac. Sci. Technol., A*, 1997, vol. 15 (2), pp. 421-27.
6. Y. Sun, T. Bell, Z. Kolosvary, and J. Flis: *Heat Treating Met*., 1999, vol. 1, pp. 9-16.
7. Y. Sun, X.Y. Li, and T. Bell: *J. Mater. Sci*., 1999, vol. 34, pp. 4793-802.
8. E. Menthe and K.T. Rie: *Surf. Coating Technol*., 1999, vols. 116–119, pp. 199-204.
9. C. Blawert, B.L. Mordike, G.A. Collins, K.T. Short, Y. Jirásková, O. Schneeweiss, and V. Perina: *Surf. Coating Technol*., 2000, vols. 128–129, pp. 219-25.
10. M.P. Fewell, D.R.G. Mitchell, J.M. Priest, K.T. Short, and G.A. Collins: *Surf. Coating Technol*., 2000, vol. 131, pp. 300-06.
11. T. Bell and K. Akamatsu: *Stainless Steel 2000—Thermochemical Surface Engineering of Stainless Steel*, Maney Publishing, London, 2001.
12. T. Christiansen and M.A.J. Somers: *Scripta Mater*., 2004, vol. 50, pp. 35-37.
13. M.A.J. Somers, T. Christiansen, and P. Møller: Danish Patent DK174707 B1 and PCT/DK03/00497.
14. D.K. Inia, A.M. Vredenberg, D.O. Boerma, F.D. Tichelaar, H. Schut, and A. van Veen: *J. Mater. Res*., 1999, vol. 14 (6), pp. 2674-79.
15. X. Xu, L. Wang, Z. Yu, J. Qiang, and Z. Hei: *Metall. Mater. Trans. A*, 2000, vol. 31A, pp. 1193-99.
16. S. Mändl, R. Günzel, E. Richter, W. Möller, and B. Rauschenbach: *Surf. Coating Technol*., 2000, vols. 128–129, pp. 423-28.
17. P.A. Dearnley, K.L. Dahm, and G. Aldrich-Smith: In *Stainless Steel 2000—Thermochemical Surface Engineering of Stainless Steel*, T. Bell and K. Akamatsu, eds., Maney Publishing, London, 2001, pp. 317-31.
18. B.A. Shedden, F.N. Kaul, M. Samandi, and B. Window: *Surf. Coating Technol*., 1997, vol. 97, pp. 102-08.
19. E.J. Mittemeijer and M.A.J. Somers: *Surf. Eng*., 1997, vol. 13, pp. 483-97.
20. T. Christiansen and M.A.J. Somers: *Z. Metallkd*., 2006, vol. 27.
21. K.H. Jack: *Proc. R. Soc. A*, 1951, vol. 208, pp. 200-15.
22. M.A.J. Somers, R.M. Lankreijer, and E.J. Mittemeijer: *Phil. Mag. A*, 1989, vol. 59 (2), pp. 353-78.
23. D.H. Jack: *Acta Metall*., 1976, vol. 24, pp. 137-46.
24. M. Hillert: *Phase Equilibria, Phase Diagrams and Phase Transformations; Their Thermodynamic Basis*, Cambridge University Press, Cambridge, United Kingdom, 1998, pp. 462-68.
25. P. Maroevic and R.B. McLellan: *J. Phys. Chem. Solids*, 1997, vol. 58 (3), pp. 403-12.
26. M.A.J. Somers and T. Christiansen: *J. Phase Equil. Diff*., 2005, vol. 26, pp. 520-28.
27. J.C.M. Li: *Metall. Trans. A*, 1978, vol. 9A, pp. 1353-80.
28. H.J. Grabke: *Mater. Sci. Forum*, 1994, vol. 154, pp. 69-85.
29. T. Christiansen and M.A.J. Somers: *Surf. Eng*., vol. 21, pp. 445-55.
30. T. Christiansen and M.A.J. Somers: unpublished research.